CHIN. PHYS. LETT. Vol. 35, No. 4 (2018) 048801 **Express Letter**

A High-Temperature β-Phase $NaMnO_2$ Stabilized by Cu Doping and Its Na Storage Properties *

Li-Wei Jiang(蒋礼威)[1,2], Ya-Xiang Lu(陆雅翔)[1**], Yue-Sheng Wang(王跃生)[1], Li-Lu Liu(刘丽露)[1,2], Xing-Guo Qi(戚兴国)[1,2], Cheng-Long Zhao(赵成龙)[1,2], Li-Quan Chen(陈立泉)[1], Yong-Sheng Hu(胡勇胜)[1,2**]

[1]*Key Laboratory for Renewable Energy, Beijing Key Laboratory for New Energy Materials and Devices, and Beijing National Laboratory for Condensed Matter Physics, Institute of Physics, Chinese Academy of Sciences, Beijing 100190*

[2]*School of Physical Sciences, University of Chinese Academy of Sciences, Beijing 100049*

(Received 1 March 2018)

The high-temperature β-phase $NaMnO_2$ is a promising material for Na-ion batteries (NIBs) due to its high capacity and abundant resources. However, the synthesis of phase-pure β-$NaMnO_2$ is burdensome and cost-ineffective because it needs to be sintered under oxygen atmosphere at high temperature and followed by a quenching procedure. Here we first report that the pure β phase can be stabilized by Cu-doping and easily synthesized by replacing a proportion of Mn with Cu via a simplified process including sintering in air and cooling to room temperature naturally. Based on the first-principle calculations, the band gap decreases from 0.7 eV to 0.3 eV, which indicates that the electronic conductivity can be improved by Cu-doping. The designed β-$NaCu_{0.1}Mn_{0.9}O_2$ is applied as cathode in NIBs, exhibiting an energy density of 419 Wh/kg and better performance in terms of rate capability and cycling stability than those in the undoped case.

PACS: 88.80.ff, 82.47.Aa, 71.20.−b, 68.55.Nq DOI: 10.1088/0256-307X/35/4/048801

Li-ion batteries (LIBs) have been achieved huge success in portable electronic devices and electric vehicles.[1−3] However, the limited lithium resources and the increasing cost have caused some concerns of using LIBs in the area of renewable energy and smart grid in the future.[4,5] Therefore strong demand is expected in exploring LIB alternatives.

Na-ion batteries (NIBs) have been regarded as the most promising supplements to LIBs due to their abundant recourse in the Earth crust, low cost, as well as similar chemical and electrochemical properties to LIBs.[6−9] Recently, extensive attention has been paid to exploring electrode materials for NIBs,[10−17] in particular, cathode materials with various structures have been obtained, such as layered oxide $Na_{0.9}Cu_{0.22}Fe_{0.3}Mn_{0.48}O_2$,[18] Prussian blue analogue $Na_{1.72}MnFe(CN)_6$,[19] tunnel $Na_{0.66}Mn_{0.66}Ti_{0.44}O_2$,[20] NASICON-type $Na_3V_2(PO_4)_3$[21] and so on, among which layered oxides have gained extensive investigation due to their two-dimensional Na^+ ion transport channel and flexibility of material design.[22−25]

Among the layered oxide cathode candidates, the high-temperature (HT) phase β-$NaMnO_2$ is of great interest because of its large specific capacity and easily accessible resources.[25] According to the literature,[25−26] β-$NaMnO_2$ is of an HT phase and exhibits much better cycle and rate performance than low-temperature (LT) phase α-$NaMnO_2$. However, the synthesis of HT β phase is very complex due to its unfavorable energy compared to the LT α phase.[27] In this study, we first report that the pure β phase could be stabilized by Cu-doping and obtained through a very simple synthesis process including sintering in air and cooling to room temperature naturally. The as-prepared β-$NaCu_{0.1}Mn_{0.9}O_2$ can be applied as cathodes in NIBs, delivering a reversible capacity of 146 mAh/g with a high initial Coulombic efficiency of 94.1% and a high capacity retention of 80.1% over 100 cycles at 10 mA/g.

The designed β-$NaCu_{0.1}Mn_{0.9}O_2$ was prepared by a simple solid-state reaction using precursors of Na_2CO_3 (99%), CuO and Mn_2O_3 (99.5%). The starting materials were ground in an agate mortar and pressed into pellets under pressure of 12 MPa. Then the pellets were heated at 950°C for 15 h in an alumina crucible and naturally cooled to room temperature. The samples were then transferred to an Ar-filled glove box. The crystalline structures were characterized by x-ray diffraction (XRD) equipment with a Bruker D8 Advance diffractometer in a transition mode using Cu K_α radiation. Chemical analysis was performed by inductively coupled plasma (ICP) emission spectroscopy. X-ray photoelectron spectra (XPS) were recorded with a spectrometer having Mg/Al K_α radiation (ESCALAB 250 Xi, ThermoFisher). All binding energies reported were corrected using the signal of carbon at 284.8 eV as an internal standard. The electrodes were fabricated by mixing 60 wt% active materials with 30 wt%

*Supported by the National Key Technologies R&D Program of China under Grant No 2016YFB0901500, and the National Nature Science Foundation of China under Grant Nos 51725206 and 51421002.

**Corresponding author. Email: yxlu@iphy.ac.cn; yshu@iphy.ac.cn

© 2018 Chinese Physical Society and IOP Publishing Ltd

acetylene black and 10 wt% polytetrafluoroethylene (PTFE, Aldrich) in an Ar-filled glove box. Typical electrode active material loadings were about 5–6 mg/cm^2. Electrodes were assembled into coin cells (CR2325 type) with a sodium metal counter electrode and an electrolyte solution composed of 1 M $NaClO_4$ in ethylene/carbonate/propylene carbonate/dimethyl carbonate (weight ratio=1:1:1).

First-principle calculations are performed with the Vienna *ab initio* simulation package (VASP).[28–29] The present data are obtained using the spin-polarized generalized gradient approximation with a parameterized exchange-correlation functional according to Perdew-PBE.[30] The Na($2p, 3s$), Mn($3d, 4s$), Cu($3d, 4s$) and O($2s, 2p$) orbitals are treated as the valence states. The strong correlation effect of transition metal is addressed with the Hubbard U correction to density functional theory (DFT) (GGA+U).[28] The effective single parameters of U–J for Mn and Cu are 4.0 eV and 7.0 eV, respectively, according to the previous work.[31–32] For all calculations the cutoffs of wave function are 520 eV. The energy and force convergence criterion are 10^{-6} eV and 0.01 eVÅ^{-1}, respectively. The calculations for electronic structures and average voltages are performed with ($2a\times b\times 2c$) supercells (including 32 atoms in total) for both of β-$NaMnO_2$ and β-$NaCu_{1/8}Mn_{7/8}O_2$. The average voltages are calculated based on the model that all Na atoms in the materials have been extracted.

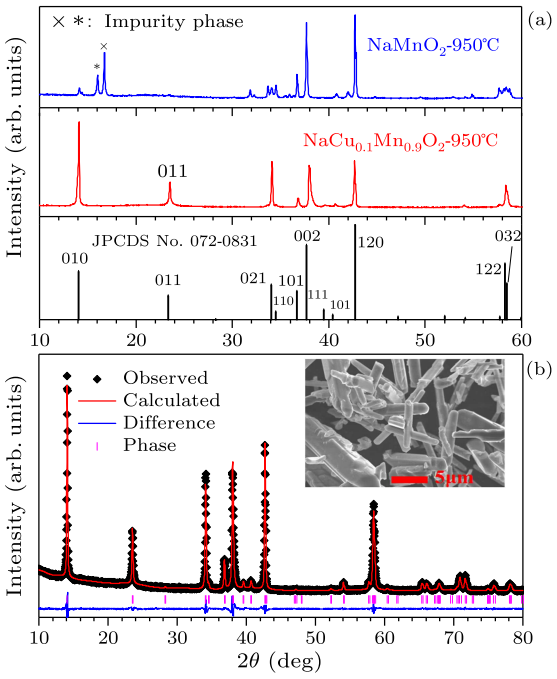

Fig. 1. (a) X-ray diffraction patterns of $NaMnO_2$ and $NaCu_{0.1}Mn_{0.9}O_2$. (b) Retrieved refinement of the as-prepared $NaCu_{0.1}Mn_{0.9}O_2$ sample. The black (red) line represents the experimental (calculated) data. The residual discrepancy is shown in blue. The inset is schematic illustration the typical scanning electron micrograph of the as-prepared $NaCu_{0.1}Mn_{0.9}O_2$ sample (scale bar is 5 μm).

Table 1. Expected and experimental sub-indexes per molecular formula for $NaCu_{0.1}Mn_{0.9}O_2$ determined by ICP measurements.

	Na	Cu	Mn
Expected mole ratio	1	0.1	0.9
Experimental mole ratio	0.9818	0.0909	0.9091

Figure 1(a) presents the x-ray diffraction (XRD) patterns of $NaCu_xMn_{1-x}O_2$ (x = 0, 0.1) synthesized by the process of sintering at 950℃ in air for 15 hours and cooling to room temperature naturally. For x = 0, namely the undoped sample, impure phases can be clearly observed. In fact, it needs very complex procedures to prepare the pure phase β-$NaMnO_2$, which is detailed in the literature[25] that the precursors must be calcined at 950℃ under oxygen atmosphere for 24 h and then immediately quenched to room temperature, which should be repeated twice. Retrieved refinement of the as-prepared $NaCu_{0.1}Mn_{0.9}O_2$ sample is shown in Fig. 1(b), and the stick morphology with length of 4–10 μm is presented in the inset. Interestingly, all of the diffraction peaks in the retrieved pattern are in good agreement with the JCPDS No. 072-0831 of β-$NaMnO_2$, indicating that the obtained structure is a pure β phase stabilized by Cu-doping. In order to confirm the composition of the as-prepared sample, ICP measurement was performed and the result indicates that the composition is $Na_{0.98}Cu_{0.09}Mn_{0.91}O_2$, which is close to the designed one, as shown in Table 1. It is worth noting that a (011) diffraction peak could be observed near 23° in $NaCu_{0.1}Mn_{0.9}O_2$, which did not appear in reported β-$NaMnO_2$ due to the existence of planar defects, thus the achieved Cu-doped sample is a more perfect β phase.[25]

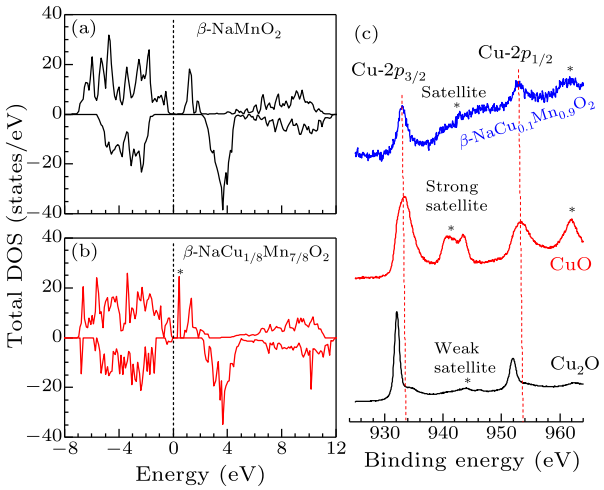

Fig. 2. Calculated total density of states (DOS) for (a) β-$NaMnO_2$ (b) β-$NaCu_{1/8}Mn_{7/8}O_2$. The Fermi levels are both set to be at 0 eV. Compared to β-$NaMnO_2$, some new states above the Fermi level for β-$NaCu_{1/8}Mn_{7/8}O_2$ are marked with star sign. (c) XPS spectra of Cu 2p for the $NaCu_{0.1}Mn_{0.9}O_2$, CuO and Cu_2O samples.

Figure 2(a) presents the total density of states (DOS) for the β-$NaMnO_2$, indicating that it is a semi-

conductor with an energy gap of 0.7 eV, which is in good agreement with the previous work.[33] Upon Cu-doping, some new states marked with asterisk above the Fermi level appear in the β-$NaCu_{1/8}Mn_{7/8}O_2$, as shown in Fig. 2(b). Obviously, the energy gap decreases from 0.7 eV to 0.3 eV, which indicates that the electronic conductivity can be improved by Cu-doping. Assuming the same charge carrier concentration and a simple Arrhenius-like relationship,[34] the electronic conductivity contributed by thermal excitation of electron at room temperature for β-$NaCu_{1/8}Mn_{7/8}O_2$ is about 10^6 times larger than that of β-$NaMnO_2$. It is interesting to know whether the valence state of Cu is monovalent or bivalent in the Cu-doped sample. Figure 2(c) presents the comparison of XPS patterns for β-$NaCu_{0.1}Mn_{0.9}O_2$, CuO and Cu_2O samples, indicating that the valence state of Cu is bivalent. In fact, the calculated magnetic moment of Cu in β-$NaCu_{1/8}Mn_{7/8}O_2$ is about $0.65\mu_B$, which also indicates that Cu is bivalent not monovalent. When a proportion of Mn^{3+} is replaced with Cu^{2+}, it would produce the same proportion of Mn^{4+} that possesses magnetic moment of $3.3\mu_B$.

Table 2. The key performance comparison of β-$NaCu_{0.1}Mn_{0.9}O_2$ and β-$NaMnO_2$.

	Discharge capacity at 1st cycle	Columbic efficiency at 1st cycle	Retention after 100 cycles at 10 mA/g	Calculated average voltage
β-$NaMnO_2$[25]	190 mAh/g	88.3%	68.4%	2.99 V
β-$NaCu_{0.1}Mn_{0.9}O_2$	146 mAh/g	94.1%	80.1%	3.07 V

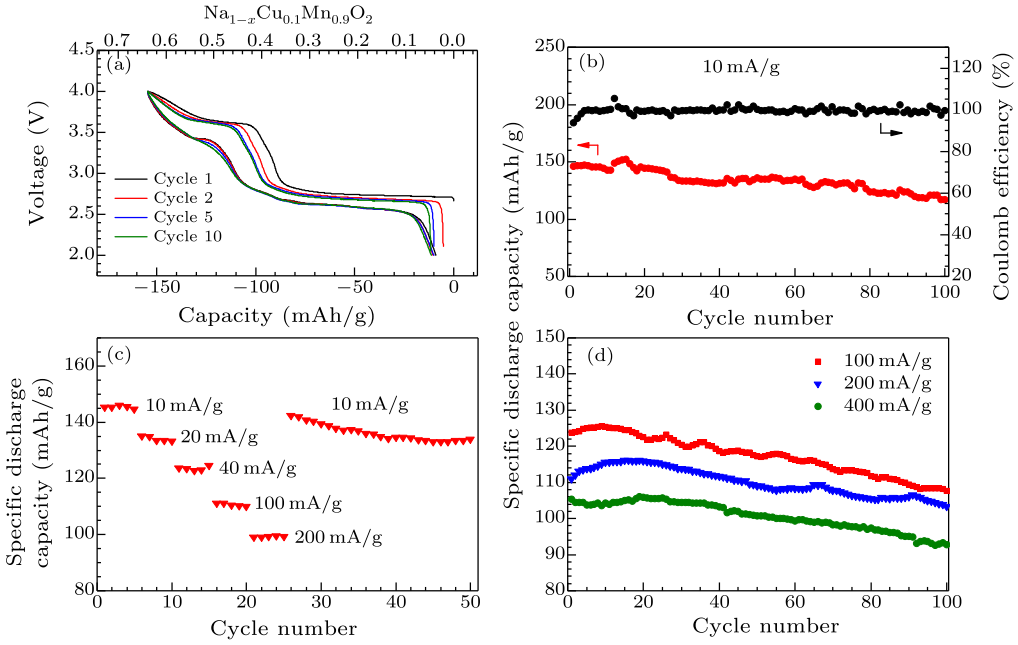

Fig. 3. (a) Charge/discharge curves for $NaCu_{0.1}Mn_{0.9}O_2$ at a rate of C/20 (10 mA/g) in the voltage range of 2.0–4.0 V versus Na^+/Na. The 1st, 2nd, 5th, and 10th Na extraction/reinsertion cycles are represented in black, red, blue and green, respectively. (b) The capacity and Coulombic efficiency versus cycle number at 10 mA/g for $NaCu_{0.1}Mn_{0.9}O_2$. (c) Rate capability of the $NaCu_{0.1}Mn_{0.9}O_2$ electrode material. (d) The capacity versus cycle number at 100 mA/g, 200 mA/g, 400 mA/g for $NaCu_{0.1}Mn_{0.9}O_2$.

As shown in Fig. 3(a), the 1st discharge capacity of β-$NaCu_{0.1}Mn_{0.9}O_2$ is 146 mAh/g, corresponding to 0.6 Na reversible intercalation deintercalation with an initial Coulombic efficiency of 94.1%, which is larger than that of β-$NaMnO_2$.[25] The energy density calculated based on cathode mass can be as high as 419 Wh/kg, which is larger than those of many other cathode materials.[18,22] It is worth pointing out that β-$NaCu_{0.1}Mn_{0.9}O_2$ exhibits excellent reversibility at the voltage plateau of about 3.5 V whereas β-$NaMnO_2$ is irreversible at all.[25] What's more, the average voltage could be lifted by Cu-doping based on the first-principle calculations as shown in Table 2, which is consistent with the experimental result.[25] Figure 3(b) presents the cycling stability of β-$NaCu_{0.1}Mn_{0.9}O_2$, indicating that 80.1% of the initial capacity is retained after 100 cycles, which is better than 68.4% retention of β-$NaMnO_2$.[25] One of the reasons for this phenomenon may be that the local structure rearrangements occurring in the planar defects of β-$NaMnO_2$ upon cycling do not appear in the β-$NaCu_{0.1}Mn_{0.9}O_2$ without planar defects.[35] The rate capability is shown in Fig. 3(c), demonstrating that the capacity is 146 mAh/g,

135 mAh/g, 124 mAh/g, 111 mAh/g, 100 mAh/g at 10 mA/g, 20 mA/g, 40 mA/g, 100 mA/g, 200 mA/g, respectively. The long-cycle performance of β-$NaCu_{0.1}Mn_{0.9}O_2$ electrode at different rates is shown in Fig. 3(d), which displays that the capacity of β-$NaCu_{0.1}Mn_{0.9}O_2$ is 123 mAh/g, 110 mAh/g, 105 mAh/g at 100 mA/g, 200 mA/g, 400 mA/g, corresponding to 87%, 92%, 87% retention after 100 cycles, respectively. The capacity at 400 mA/g for β-$NaCu_{0.1}Mn_{0.9}O_2$ is 105 mAh/g, which is larger than 91 mAh/g of β-$NaMnO_2$, indicating that β-$NaCu_{0.1}Mn_{0.9}O_2$ has better rate capability than that of β-$NaMnO_2$.[25] Table 2 lists the key performance comparison of β-$NaMnO_2$ and β-$NaCu_{0.1}Mn_{0.9}O_2$. The lower capacity of β-$NaCu_{0.1}Mn_{0.9}O_2$ could be attributed to the content decrease of Mn^{3+} in the Cu-doped sample. Obviously, except for the lower capacity, β-$NaCu_{0.1}Mn_{0.9}O_2$ presents many other advantages over β-$NaMnO_2$ such as higher initial Coulombic efficiency, higher average voltage, as well as better rate capability and cycle performance.

In summary, a pure HT β phase is stabilized through Cu-doping in $NaMnO_2$, and could be achieved via a simplified synthesis process without the oxygen atmosphere and quenching step. The designed β-$NaCu_{0.1}Mn_{0.9}O_2$ can be applied as cathodes in NIBs and can exhibit superior performance. Compared with the undoped sample, the Cu-doping cathode demonstrates a higher initial Coulombic efficiency, higher average voltage, as well as better rate capability and cycling stability. With the assist of structural characterizations and DFT calculations, it is revealed that the obtained superior performance could be attributed to the pure β phase without planar defects stabilized by Cu-doping together with the higher electronic conductivity due to the narrower band gap. In general, Cu-doping strategy is very promising for the stabilization of HT β phase and the fundamental reasons for this is under investigation.

References

[1] Mizushima K, Jones P C, Wiseman P J and Goodenough J B 1980 *Mater. Res. Bull.* **15** 783
[2] Arm M and Tarascon J M 2008 *Nature* **451** 652
[3] Zu C X and Li H 2011 *Energy Environ. Sci.* **4** 2614
[4] Su H, Jaffer S and Yu H 2016 *Energy Storage Mater.* **5** 116
[5] Slater M D, Kim D, Lee E and Johnson C S 2013 *Adv. Funct. Mater.* **23** 947
[6] Li Y, Lu Y, Zhao C, Hu Y, Titirici M, Li H, Huang X and Chen L 2017 *Energy Storage Mater.* **7** 130
[7] Kim S W, Seo D H, Ma X H, Ceder G and Kang K 2012 *Adv. Energy Mater.* **2** 710
[8] Komaba S, Murata W, Ishikawa T, Yabuuchi N, Ozeki T, Nakayama T, Ogata A, Gotoh K and Fujiwara K 2011 *Adv. Funct. Mater.* **21** 3859
[9] Li Y, Hu Y, Qi X, Rong X, Li H, Huang X and Chen L 2016 *Energy Storage Mater.* **5** 191
[10] Xu S, Wang Y, Ben L, Lyu Y, Song N, Yang Z, Li Y, Mu L, Yang H, Gu L, Hu Y, Li H, Cheng Z, Chen L and Huang X 2015 *Adv. Energy Mater.* **5** 201501156
[11] Zhao L, Zhao J, Hu Y S, Li H, Zhou Z, Arm, M and Chen L 2012 *Adv. Energy Mater.* **2** 962
[12] Yabuuchi, Naoaki, Kubota Kei, Dahbi Mouad and Komaba Shinichi 2013 *Chem. Rev.* **113** 6552
[13] Sun Y, Zhao L, Pan H, Lu X, Gu L, Hu Y S, Li H, Arm, M, Ikuhara Y, Chen L and Huang X 2013 *Nat. Commun.* **4** 1870
[14] Pan H, Lu X, Yu X, Hu Y S, Li H, Yang X Q and Chen L 2013 *Adv. Energy Mater.* **3** 1186
[15] Wang Y, Yu X Q, Xu S Y, Bai J, Xiao R J, Hu Y S, Li H, Yang X Q, Chen L Q and Huang X J 2013 *Nat. Commun.* **4** 2365
[16] Qi X, Wang Y, Jiang L, Mu L, Zhao C, Liu L, Hu Y S and Chen L 2016 *Part. Part. Syst. Charact.* **33** 538
[17] Rong X, Liu J, Hu E, Liu Y, Wang Y, Wu J, Yu X, Page K, Hu Y, Yang X, Chen L and Huang X 2018 *Joule* **2** 125
[18] Mu L, Xu S, Li Y, Hu Y, Li H, Chen L and Huang X 2015 *Adv. Mater.* **27** 6928
[19] Wang L, Lu Y H, Liu J, Xu M W, Cheng J G, Zhang D W and Goodenough J B 2013 *Angew. Chem. Int. Ed.* **52** 1964
[20] Wang Y, Mu L, Liu J, Yang Z, Yu X, Gu L, Hu Y S, Li H, Yang X, Chen L and Huang X 2015 *Adv. Energy Mater.* **5** 1501005
[21] Jian Z, Han W, Lu X, Yang H, Hu Y S, Zhou J, Zhou Z, Li J, Chen W, Chen D and Chen L 2013 *Adv. Energy Mater.* **3** 156
[22] Li Y, Yang Z, Xu S, Mu L, Gu L, Hu Y, Li H and Chen L 2015 *Adv. Sci.* **2** 1500031
[23] Xu S, Wu X, Li Y, Hu Y and Chen L 2014 *Chin. Phys.* B **23** 118202
[24] Mu L, Hu Y and Chen L 2015 *Chin. Phys.* B **24** 038202
[25] Billaud J, Cleíment R J, Armstrong A R, Canales V J, Rozier P, Grey C P and Bruce P G 2014 *J. Am. Chem. Soc.* **136** 17243
[26] Mendiboure A, Delmas C and Hagenmuller P 1971 *Solid State Chem.* **3** 1
[27] Velikokhatnyi O, Chang C and Kumta P 2003 *J. Electrochem. Soc.* **150** A1262
[28] Kresse G and Furthmüller J 1996 *Phys. Rev.* B **54** 11169
[29] Shi S, Gao J, Liu Y, Zhao Y, Wu Q, Ju W, Ouyang C and Xiao R 2016 *Chin. Phys.* B **25** 018212
[30] Anisimov V, Zaanen J and Andersen O 1991 *Phys. Rev.* B **44** 943
[31] Perdew J, Burke K and Ernzerhof M 1996 *Phys. Rev. Lett.* **77** 3865
[32] Nolan M and Elliott S D 2006 *Phys. Chem. Chem. Phys.* **8** 5350
[33] Wang Z, Chen Y and Ouyang C 2014 *Phys. Lett.* A **378** 2449
[34] Ong S, Chevrier V and Ceder G 2011 *Phys. Rev.* B **83** 075112
[35] Cleímnt R, Middlemiss D, Seymour I, Ilott A and Grey C 2016 *Chem. Mater.* **28** 8228